Nonlinear Behaviour of Damaged Concrete Bridge Structures under Moving Vehicular Loads

X. Q. ZHU* D. Q. CAO** S. S. LAW*** and J. Z. PAN**
*School of Engineering, University of Western Sydney,
Locked Bag 1797, Penrith, NSW 2751, Australia
E-mail: xinqun.zhu@uws.edu.au
**School of Astronautics, Harbin Institute of Technology
P.O. Box 137, Harbin 150001, P.R. China
***Department of Civil and Structural Engineering, Hong Kong Polytechnic University,
Hunghom, Kowloon, Hong Kong

Abstract
Recently, there has been increased interest in using non-linear vibration techniques to detect damage in concrete bridge structures. It is necessary to understand the nonlinear behavior of concrete structures under vibration loading for damage detection. In this paper, a damage beam element is developed to analyze the non-linear dynamic behavior of damaged concrete bridge structures subject to moving vehicular loads. The damage is modeled as a combination of a rotational spring and shear effect due to the concrete cracking and local bond deterioration of the concrete-steel interface. Numerical simulations are presented to study the damage effects on the dynamic behavior of concrete bridge structures under moving vehicular loads. The results show that the model is reliable and effective to describe the damage in the concrete bridge structures.

Key words: Nonlinear, Damage, Moving loads, Concrete structures

1. Introduction

In view of long-term health monitoring requirements of structures, such as bridges, it is desirable to have the damage detection techniques including the operating loads, such as vehicular loads, as excitation source. The occurrence of damage in a structure produces changes in its dynamic behaviour. An understanding of these changes can lead to the detection, location and the characterization of the extent of the damage. Mazurek and Dewolf conducted laboratory studies on a simple two-span girder under moving loads in their structural deterioration study using vibration signature analysis[1]. Structural damage was artificially introduced by release of supports and insertion of cracks. Lee and Ng used the assumed mode method to analyze the dynamic response of a beam with a single-sided crack subject to a moving load on the top[2]. The beam is modelled as two segments separated by the crack. Two different sets of admissible functions satisfying the respective geometric boundary conditions are then assumed for these two fictitious sub-beams. The rotational discontinuity at the crack is modelled by a torsional spring with an equivalent spring constant for the crack. The equality of transverse deflection at the crack is enforced by a linear spring of very large stiffness. Parhi and Behera utilized an analytical method along with the experimental verification to investigate the behaviour of a cracked beam with a moving mass[3]. A local stiffness matrix was used to model the crack section. Mahmoud

and Abou Zaid analyzed the effect of crack size on the dynamic behaviour of simply-supported undamped Bernoulli-Euler beams subjected to a moving mass[4]. The presence of crack results in higher deflections and alters the beam response pattern. Bilello and Bergman presented a theoretical and experimental study of the response of a damaged Euler-Bernoulli beam traversed by a moving mass[5]. Damage is modeled through rotational springs whose compliance is evaluated using linear elastic fracture mechanics. Lee et al presented an experimental study on bridge health-monitoring using ambient vibration by ordinary traffic loadings[6]. The assessment of damage locations and severities was carried out based on the estimated modal parameters using the neural networks technique. A time-domain approach was also developed to detect the damage in beam structures using vibration data with a moving oscillator as an excitation source by Majumder and Manohar [7]. All above studies use the open crack model with the linear assumption.

Since reinforced concrete structures are nonlinear in behavior, important information is lost when the linear assumption is made. Kato and Shimada presented the vibration measurement on an existing prestressed concrete bridge deck during its failure test[8]. The decrement of natural frequency was small even if cracks occurred while the prestressed steel wires were in the elastic state. The cracks of concrete were closed together by the effective prestressing after the load was removed. Eccles et al presented the phase-plane plot generated by exciting the beam at a natural frequency with constant excitation energy[9]. The degree to which the plot deviates from a circle is a measure of the nonlinearity of the system, and the absolute change in the natural frequencies is used as a damage indicator. Van Den Abeele and De Visscher performed both linear and nonlinear acoustical experiments on a reinforced concrete beam in which damage is gradually induced by means of static loading[10]. The tests demonstrated that although the beam did not behave linearly when undamaged, once the beam was damaged using four-point loading the non-linearities became far more pronounced. Owen et al applied auto-regressive time series modelling for the time-frequency analysis of civil engineering structures[11]. The data includes non-stationary data obtained from the large amplitude response of a cable stayed bridge to wind excitation and non-linear data obtained from the modal testing of a cracked reinforced concrete beam. Neild et al measured and analyzed the stiffness across a cracked region of a reinforced concrete beam over a cycle of static loads with four possible non-linear mechanisms which resulted in amplitude-dependent natural frequencies[12]. Neild et al also studied the nonlinear vibration characteristics by conducting impact excitation vibration tests on reinforced concrete beams at increasing levels of crack damage[13]. Law and Zhu presented an experimental study on a Tee-section reinforced concrete beam subject to the action of a moving model vehicle in laboratory[14]. Nonlinearities are detected by examining the changes in the natural frequency when the vehicular loads are at different locations along the beam.

In this paper, a damage beam element is developed to analyze the non-linear dynamic behavior of damaged concrete bridge structures subject to moving vehicular loads. The damage is modeled as a combination of a rotational spring and shear effect due to the concrete cracking and local bond deterioration of the concrete-steel interface. Numerical simulations are presented to study the damage effects on the dynamic behavior of concrete bridge structures under moving vehicular loads. The results show that the model is reliable and effective to describe the damage in the concrete bridge structures.

2. Damage Beam Elements

2.1 Rotational Spring Model

The rotational spring model is widely used to study cracked beams, in which the effect of structural damage is modeled through a local compliance[4][5]. Since reinforced concrete structures are nonlinear in behavior, important information is lost when the linear

assumption is made. There are many existing hysteretic models to describe the deterioration in the structures, especially for inelastic structures[15]. According to Richard and Abbott's hysteretic model[16], the moment-rotation relation at the damage point can be written as follow.

$$M = \left[1 - \alpha_r + \frac{\alpha_r}{\left[1 + \left| \frac{\alpha_r k_0 |\theta|}{M_0} \right|^n \right]^{1/n}} \right] k_0 |\theta| \tag{1}$$

and the corresponding tangent stiffness by

$$K_{rd} = \frac{dM}{d\theta} = \left[1 - \alpha_r + \frac{\alpha_r}{\left[1 + \left| \frac{\alpha_r k_0 |\theta|}{M_0} \right|^n \right]^{(n+1)/n}} \right] k_0 \tag{2}$$

where k_0 is the initial rotational stiffness, $|\theta|$ is the slip angle (i.e. the rotation of the connection) equal to the difference between the angles at the two ends of a connection, $|\theta| = |\theta_d^L - \theta_d^R|$, α_r is the damage indicator which is defined as the ratio between the stiffness reduction due to concrete cracking and local bond deterioration of the concrete-steel interface to the initial stiffness and there is no damage when $\alpha_r = 0$, M_0 is a reference moment related to the yield moment and n is a parameter defining the sharpness of the curve and controlling the smoothness of the transition from elastic to inelastic range. When $n \to \infty$, the model reduces to a bilinear system.

2.2 Bond-slip Model

Concrete is a brittle materials in which micro and potential cracks are pervasive. The observations using scanning electron microscope showed that the interface between the concrete and steel was always surrounded by micro-cracks. When the micro-crack is formed, debonding takes place, or a large slip occurs, the load-transferring capacity of the interface between concrete and steel will drop dramatically. Energy dissipated by the friction resulting from the interfacial relative displacement due to crack opening and closing. Here an equivalent model at damage point is used to describe the concrete-steel interface behavior. The model consists of three parameters basing on the load-deflection relation[17] as

$$Q = (1 - \alpha_s) Q_s \frac{K_0 w}{\left(Q_s^m + (K_0 w)^m \right)^{1/m}} \tag{3}$$

where Q_s is the ultimate friction capacity of connection which is equivalent to the characteristic frictional bond-stress value of the undamaged beam. α_s is a scalar damage indicator and there is no damage when $\alpha_s = 0$. K_0 is the initial connection stiffness of undamaged beam and m is the shape parameter of Q-w curve. When $m \to \infty$, the model is also a bilinear system. The corresponding instantaneous stiffness by

$$K_{sd} = \frac{dQ}{dw} = (1 - \alpha_s) K_0 \left[1 - \frac{(K_0 w)^m}{(K_0 w)^m + Q_s^m} \right]^{(m+1)/m} \tag{4}$$

2.3 Damage Beam Element

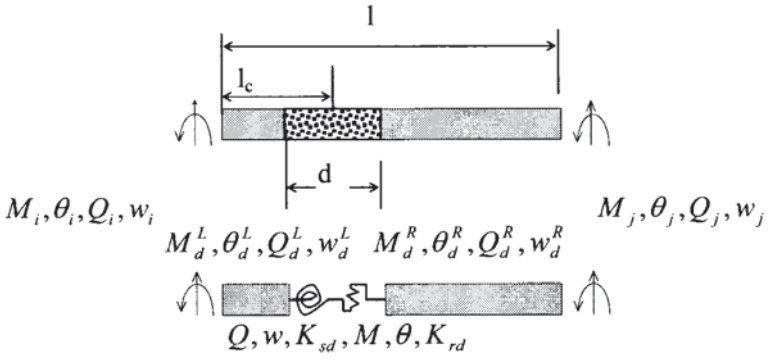

Fig. 1 Cracked beam element

Figure 1 shows a prismatic isotropic beam element of length l with a damage zone which is located at l_c ($l_c \neq 0$) from left end. The damaged beam element is modeled as two segment beam connected by a virtual spring. Assuming the rigidity of undamaged beam is EI, the stiffness matrices link up the force and deformation at the ends of two segment beams are as follow

$$\begin{Bmatrix} Q_i \\ M_i \\ Q_d^L \\ M_d^L \end{Bmatrix} = \frac{EI}{l_1^3}\begin{bmatrix} 12 & 6l_1 & -12 & 6l_1 \\ 6l_1 & 4l_1^2 & -6l_1 & 2l_1^2 \\ -12 & -6l_1 & 12 & -6l_1 \\ 6l_1 & 2l_1^2 & -6l_1 & 4l_1^2 \end{bmatrix}\begin{Bmatrix} w_i \\ \theta_i \\ w_d^L \\ \theta_d^L \end{Bmatrix} \tag{5}$$

$$\begin{Bmatrix} Q_d^R \\ M_d^R \\ Q_j \\ M_j \end{Bmatrix} = \frac{EI}{(l-l_2)^3}\begin{bmatrix} 12 & 6(l-l_2) & -12 & 6(l-l_2) \\ 6(l-l_2) & 4(l-l_2)^2 & -6(l-l_2) & 2(l-l_2)^2 \\ -12 & -6(l-l_2) & 12 & -6(l-l_2) \\ 6(l-l_2) & 2(l-l_2)^2 & -6(l-l_2) & 4(l-l_2)^2 \end{bmatrix}\begin{Bmatrix} w_d^R \\ \theta_d^R \\ w_j \\ \theta_j \end{Bmatrix} \tag{6}$$

where $w_i, w_j, \theta_i, \theta_j$ are the displacements and rotations of two nodes, Q_i, Q_j, M_i, M_j are the corresponding lateral shear forces and moments at two nodes of the element, $w_d^L, \theta_d^L, w_d^R, \theta_d^R$ are the two end displacements and rotations of the spring, $Q_d^L, M_d^L, Q_d^R, M_d^R$ are the corresponding shear forces and moments at two ends of the spring. d is the length of the damage zone. $l_1 = l_c - d/2, l_2 = l - l_c - d/2$.

According to the three basic governing conditions, i.e. the compatibility, the equilibrium and the constitutive relations for the spring, the connection matrix of the spring is given as follow

$$\begin{Bmatrix} Q_d^L \\ M_d^L \\ Q_d^R \\ M_d^R \end{Bmatrix} = \begin{bmatrix} K_{sd} & 0 & -K_{sd} & 0 \\ 0 & K_{rd} & 0 & -K_{rd} \\ -K_{sd} & 0 & K_{sd} & 0 \\ 0 & -K_{rd} & 0 & K_{rd} \end{bmatrix}\begin{Bmatrix} w_d^L \\ \theta_d^L \\ w_d^R \\ \theta_d^R \end{Bmatrix} \tag{7}$$

where K_{sd}, K_{rd} are the shear and rotational stiffness of the spring.

Substitute Eq. (7) into Eqs. (5) and (6), the stiffness matrix of the damaged beam element can be given as

$$\mathbf{F} = \mathbf{K_d q} \tag{8}$$

where $\mathbf{F} = \{Q_i \quad M_i \quad Q_j \quad M_j\}^T$, $\mathbf{q} = \{w_i \quad \theta_i \quad w_j \quad \theta_j\}^T$,

$$\mathbf{K_d} = \mathbf{K_1} + \mathbf{K_2}\mathbf{K_3}^{-1}\mathbf{K_4} \tag{9}$$

where

$$\mathbf{K}_1 = EI\begin{bmatrix} 12/l_1^3 & 6/l_1^2 & 0 & 0 \\ 6/l_1^2 & 4/l_1 & 0 & 0 \\ 0 & 0 & 12/(l-l_2)^3 & -6/(l-l_2)^2 \\ 0 & 0 & -6/(l-l_2)^2 & 4/(l-l_2) \end{bmatrix}$$

$$\mathbf{K}_2 = EI\begin{bmatrix} -12/l_1^3 & 6/l_1^2 & 0 & 0 \\ -6/l_1^2 & 2/l_1 & 0 & 0 \\ 0 & 0 & -12/(l-l_2)^3 & -6/(l-l_2)^2 \\ 0 & 0 & 6/(l-l_2)^2 & 2/(l-l_2) \end{bmatrix}$$

$$\mathbf{K}_3 = \begin{bmatrix} K_{sd} & 0 & -K_{sd} & 0 \\ 0 & K_{rd} & 0 & -K_{rd} \\ -K_{sd} & 0 & K_{sd} & 0 \\ 0 & -K_{rd} & 0 & K_{rd} \end{bmatrix} - EI\begin{pmatrix} 12/l_1^3 & -6/l_1^2 & 0 & 0 \\ -6/l_1^2 & 4/l_1 & 0 & 0 \\ 0 & 0 & 12/(l-l_2)^3 & 6/(l-l_2)^2 \\ 0 & 0 & 6/(l-l_2)^2 & 4/(l-l_2) \end{pmatrix}$$

$$\mathbf{K}_4 = EI\begin{bmatrix} -12/l_1^3 & -6l/l_1^2 & 0 & 0 \\ 6l/l_1^2 & 2l^2/l_1 & 0 & 0 \\ 0 & 0 & -12/(l-l_2)^3 & 6/(l-l_2)^2 \\ 0 & 0 & -6/(l-l_2)^2 & 2/(l-l_2) \end{bmatrix} \tag{10}$$

2.4 Element Damage Index

In the inverse problem of damage identification, it is assumed that the stiffness matrix of the whole element decreases uniformly with damage, and the flexural rigidity, EI, becomes $(1-\alpha)EI$ when there is a damage, and α is the damage index. The fractional change in stiffness of an element can be expressed as

$$\Delta K_e = \left(K_e - \tilde{K}_e\right) = \alpha K_e \tag{11}$$

$$K_e = \frac{EI}{l^3}\begin{bmatrix} 12 & 6l & -12 & 6l \\ 6l & 4l^2 & -6l & 2l^2 \\ -12 & -6l & 12 & -6l \\ 6l & 2l^2 & -6l & 4l^2 \end{bmatrix} \tag{12}$$

where K_e and $\tilde{K}_e$ are the element stiffness matrices of undamaged and damage beam element, l is length of the beam element. ΔK_e is the stiffness reduction of the element. A positive value of $\alpha \in [0,1]$ will indicate a loss in the element stiffness. The element is undamaged when $\alpha = 0$ and the stiffness of element is completely lost when $\alpha = 1$.

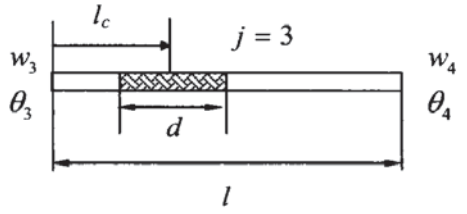

Fig.2 The third element of bridge

$$\begin{Bmatrix} Q_d^L \\ M_d^L \\ Q_d^R \\ M_d^R \end{Bmatrix} = kd \begin{Bmatrix} w_d^L \\ \theta_d^L \\ w_d^R \\ \theta_d^R \end{Bmatrix} =$$

$$(1-\alpha)EI \begin{bmatrix} \frac{12}{l_1^3}+\frac{12}{(l-l_2)^3} & \frac{6}{l_1^2}+\frac{6}{(l-l_2)^2} & -\frac{12}{l_1^3}-\frac{12}{(l-l_2)^3} & \frac{6}{l_1^2}+\frac{6}{(l-l_2)^2} \\ \frac{6}{l_1^2}+\frac{6}{(l-l_2)^2} & \frac{4}{l_1}+\frac{4}{(l-l_2)} & -\frac{6}{l_1^2}-\frac{6}{(l-l_2)^2} & \frac{2}{l_1}+\frac{2}{(l-l_2)} \\ -\frac{12}{l_1^3}-\frac{12}{(l-l_2)^3} & -\frac{6}{l_1^2}-\frac{6}{(l-l_2)^2} & \frac{12}{l_1^3}+\frac{12}{(l-l_2)^3} & -\frac{6}{l_1^2}-\frac{6}{(l-l_2)^2} \\ \frac{6}{l_1^2}+\frac{6}{(l-l_2)^2} & \frac{2}{l_1}+\frac{2}{(l-l_2)} & -\frac{6}{l_1^2}-\frac{6}{(l-l_2)^2} & \frac{4}{l_1}+\frac{4}{(l-l_2)} \end{bmatrix} \begin{Bmatrix} w_d^L \\ \theta_d^L \\ w_d^R \\ \theta_d^R \end{Bmatrix} \tag{13}$$

As previously deduced, the same relationship can be obtained as follows

$$\mathbf{F} = \mathbf{K}_\alpha \mathbf{q} \tag{14}$$

$$\mathbf{q} = \{w_3 \quad \theta_3 \quad w_4 \quad \theta_4\}^T, \mathbf{F} = \{Q_3 \quad M_3 \quad Q_4 \quad M_4\}, \mathbf{K}_\alpha = \mathbf{K}_1 + \mathbf{K}_2 \mathbf{K}_3'^{-1} \mathbf{K}_4,$$

$$\mathbf{K}_3' = kd - EI \begin{pmatrix} 12/l_1^3 & -6/l_1^2 & 0 & 0 \\ -6/l_1^2 & 4/l_1 & 0 & 0 \\ 0 & 0 & 12/(l-l_2)^3 & 6/(l-l_2)^2 \\ 0 & 0 & 6/(l-l_2)^2 & 4/(l-l_2) \end{pmatrix} \tag{15}$$

3. Dynamic Response Analysis

3.1 Bridge-vehicle System

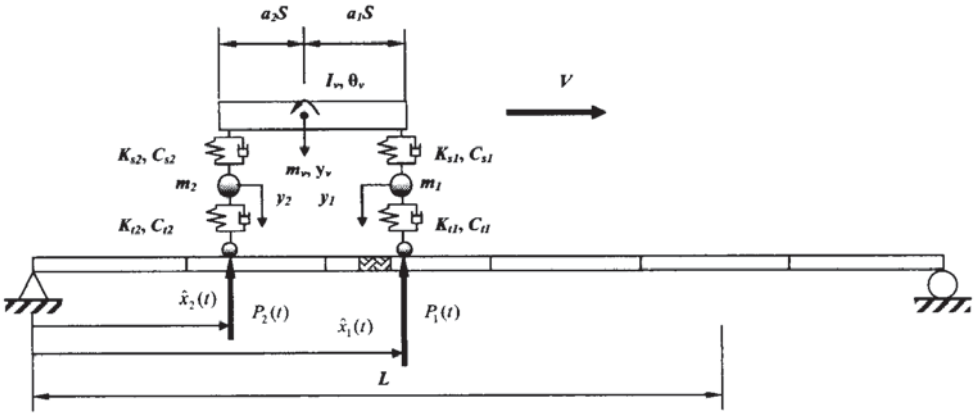

Fig.3 Bridge-vehicle system

Figure 3 shows a vehicle moving at a speed v over a bridge modelled as a half vehicle model[18]. The bridge is modelled with different number of finite elements. The equation of motion of the vehicle is derived using the Lagrange formulation as follow

$$\begin{bmatrix} M_{v1} & \mathbf{0} \\ \mathbf{0} & M_{v2} \end{bmatrix} \ddot{Y} + \begin{bmatrix} C_{v11} & C_{v12} \\ C_{v21} & C_{v22} \end{bmatrix} \dot{Y} + \begin{bmatrix} K_{v11} & K_{v12} \\ K_{v21} & K_{v22} \end{bmatrix} Y = -\begin{Bmatrix} 0 \\ P_{\text{int}} \end{Bmatrix} + \begin{Bmatrix} 0 \\ M_s \end{Bmatrix} \tag{16}$$

where $Y = \{y_v, \theta_v, y_1, y_2\}^T$ is the response vector of the vehicle; M_s is the static load of the vehicle; $M_{v1}, M_{v2}, C_{v11}, C_{v12}, C_{v21}, C_{v22}, K_{v11}, K_{v12}, K_{v21}, K_{v22}, M_s$ are the mass, damping and stiffness sub-matrices of the vehicle respectively and they are given in

Appendix I; $P_{\text{int}} = \{P_1(t), \ldots\ldots, P_{Np}(t)\}^T$ is the vehicle-bridge interaction force vector with N_p=2, and

$$\begin{cases} P_1(t) = K_{t1}(y_1 - w(\hat{x}_1(t),t) - r(\hat{x}_1(t))) + C_{t1}(\dot{y}_1 - \dot{w}(\hat{x}_1(t),t)) \\ P_2(t) = K_{t2}(y_2 - w(\hat{x}_2(t),t) - r(\hat{x}_2(t))) + C_{t2}(\dot{y}_2 - \dot{w}(\hat{x}_2(t),t)) \end{cases} \quad (17)$$

where $r(x)$ is the road surface roughness at the location of the tires; $\hat{x}_1(t), \hat{x}_2(t)$ are the positions of the front axle and rear axle respectively at time t, and g is the acceleration of gravity. $w(\hat{x}_i(t),t)$, $\dot{w}(\hat{x}_i(t),t)$ are the vertical dynamic deflection of the beam and its time derivative at the ith load at time t. $K_{t1}, K_{t2}, C_{t1}, C_{t2}$ are the stiffness and damping of the two tires respectively.

The elemental mass and stiffness matrices are obtained using the Hermitian cubic interpolation shape functions. The supporting beam structure is discretized into m-1 beam element where m is the number of nodal points. The shape functions of the jth element in its local coordinate can be obtained as follows:

$$H_j = \left\{ 1 - 3(\frac{x}{l})^2 + 2(\frac{x}{l})^3 \quad x(\frac{x}{l} - 1)^2 \quad 3(\frac{x}{l})^2 - 2(\frac{x}{l})^3 \quad x(\frac{x}{l})^2 - \frac{x^2}{l} \right\}^T \quad (18)$$

where l is the length of the beam element. With the assumption of Rayleigh damping, the equation of motion for the bridge can be written as

$$M_b\ddot{R} + C_b\dot{R} + K_bR = H_cP_{\text{int}}, \quad (19)$$

$$H_cP_{\text{int}} = \{0 \cdots H_2P_2 \cdots H_1P_1 \cdots 0\}^T \quad (20)$$

$$R = \{R_1 \ldots R_{NN}\}^T = \{w_1, \theta_1, \ldots w_{NN}, \theta_{NN}\}^T \quad (21)$$

where M_b, C_b, K_b are the mass, damping and stiffness matrices of the bridge respectively. $\ddot{R}, \dot{R}, R$ are the nodal acceleration, velocity and displacement vectors of the bridge respectively, NN is the number of degrees-of-freedom of the bridge and j is the number of finite element in the beam, here NN=2×(j+1), and H_cP_{int} is the equivalent nodal load vector from the bridge-vehicle interaction force with

$$H_c = \begin{Bmatrix} 0 & \cdots & 0 & \cdots & H_1 & \cdots & 0 \\ 0 & \cdots & H_2 & \cdots & 0 & \cdots & 0 \end{Bmatrix}^T$$

H_c is a $NN \times N_p$ matrix with zero entries except at the degrees-of-freedom corresponding to the nodal displacements of the beam elements on which the load is acting.

Combining Eqs. (16) and (19), we have

$$\begin{bmatrix} M_b & 0 & H_cM_{v2} \\ 0 & M_{v1} & 0 \end{bmatrix} \begin{Bmatrix} \ddot{R} \\ \ddot{Y} \end{Bmatrix} + \begin{bmatrix} C_b & H_cC_{v21} & H_cC_{v22} \\ 0 & C_{v11} & C_{v12} \end{bmatrix} \begin{Bmatrix} \dot{R} \\ \dot{Y} \end{Bmatrix} + \begin{bmatrix} K_b & H_cK_{v21} & H_cK_{v22} \\ 0 & K_{v11} & K_{v12} \end{bmatrix} \begin{Bmatrix} R \\ Y \end{Bmatrix} = \begin{Bmatrix} H_cM_s \\ 0 \end{Bmatrix} \quad (22)$$

To find the time response of the beam from Eq. (16), a step-by-step solution can be obtained using the Newmark direct integration method. The deflection of the bridge at position x and time t can then be expressed as

$$w(x,t) = H(x)\, R(t) \quad (23)$$

where $H(x) = \{ 0 \quad \cdots \quad H(x)_j^T \quad 0 \quad \cdots \quad 0 \}$ with $(j-1)l \le x(t) \le jl$. $H(x)$ is a $1 \times NN$ vector with zero entries except at the degrees-of-freedom corresponding to the nodal displacements of the jth beam element on which the point x is located. The components of the vector $H(x)_j$ are calculated similar to Eq. (15) with $x(t)$ replacing $\hat{x}_i(t)$.

The displacements $w_i(\hat{x}_i(t),t)$ at measurement locations $\hat{x}_1(t), \hat{x}_2(t)$ can also be obtained from the shape functions and nodal displacements of the beam as:

$$\begin{pmatrix} w_1 \\ w_2 \end{pmatrix} = H_c^T R \tag{24}$$

where H_c as mentioned before.

Substituting Eqs. (16) for (24), we have

$$\begin{bmatrix} m_1 & 0 \\ 0 & m_2 \end{bmatrix}\begin{Bmatrix} \ddot{y}_1 \\ \ddot{y}_2 \end{Bmatrix} + \begin{bmatrix} -C_{S1} & C_{S1}a_1 S \\ -C_{S2} & -C_{S2}a_2 S \end{bmatrix}\begin{Bmatrix} \dot{y}_v \\ \dot{y}_\theta \end{Bmatrix} + \begin{bmatrix} C_{S1} & 0 \\ 0 & C_{S2} \end{bmatrix}\begin{Bmatrix} \dot{y}_1 \\ \dot{y}_2 \end{Bmatrix} + \begin{bmatrix} -K_{S1} & K_{S1}a_1 S \\ -K_{S2} & -K_{S2}a_2 S \end{bmatrix}\begin{Bmatrix} y_v \\ y_\theta \end{Bmatrix}$$
$$+ \begin{bmatrix} K_{S1} & 0 \\ 0 & K_{S2} \end{bmatrix}\begin{Bmatrix} y_1 \\ y_2 \end{Bmatrix} = -\begin{bmatrix} K_{t1} & 0 \\ 0 & K_{t2} \end{bmatrix}\begin{Bmatrix} y_1 \\ y_2 \end{Bmatrix} + \begin{bmatrix} K_{t1} & 0 \\ 0 & K_{t2} \end{bmatrix}\begin{Bmatrix} w_1 \\ w_2 \end{Bmatrix} \tag{25}$$
$$- \begin{bmatrix} C_{t1} & 0 \\ 0 & C_{t2} \end{bmatrix}\begin{Bmatrix} \dot{y}_1 \\ \dot{y}_2 \end{Bmatrix} + \begin{bmatrix} C_{t1} & 0 \\ 0 & C_{t2} \end{bmatrix}\begin{Bmatrix} \dot{w}_1 \\ \dot{w}_2 \end{Bmatrix} + g\begin{bmatrix} m_1 + a_2 m_v \\ m_2 + a_1 m_v \end{bmatrix}$$

Therefore, we obtain the governing equation of the front axle and near axle : $\{y_1\ y_2\}^T$

$$M_{v2}\begin{Bmatrix} \ddot{y}_1 \\ \ddot{y}_2 \end{Bmatrix} + C_{v21}\begin{Bmatrix} \dot{y}_v \\ \dot{y}_\theta \end{Bmatrix} + C_{v22}\begin{Bmatrix} \dot{y}_1 \\ \dot{y}_2 \end{Bmatrix} + K_{v21}\begin{Bmatrix} y_v \\ y_\theta \end{Bmatrix} + K_{v22}\begin{Bmatrix} y_1 \\ y_2 \end{Bmatrix}$$
$$= -K_t\begin{Bmatrix} y_1 \\ y_2 \end{Bmatrix} + K_t H_c^T R - C_t\begin{Bmatrix} \dot{y}_1 \\ \dot{y}_2 \end{Bmatrix} + C_t H_c^T \dot{R} + M_S \tag{26}$$

For $Y_1 = \{y_v, y_\theta\}^T, Y_2 = \{y_1, y_2\}^T$, and combining Eqs. (22) and (26), the equation of the whole system is:

$$\begin{bmatrix} M_b & 0 & H_c M_{v2} \\ 0 & M_{v1} & 0 \\ 0 & 0 & M_{v2} \end{bmatrix}\begin{Bmatrix} \ddot{R} \\ \ddot{Y}_1 \\ \ddot{Y}_2 \end{Bmatrix} + \begin{bmatrix} C_b & H_c C_{v21} & H_c C_{v22} \\ 0 & C_{v11} & C_{v12} \\ -C_t H_c^T & C_{v21} & C_{v22} + C_t \end{bmatrix}\begin{Bmatrix} \dot{R} \\ \dot{Y}_1 \\ \dot{Y}_2 \end{Bmatrix} \tag{27}$$
$$+ \begin{bmatrix} K_b & H_c K_{v21} & H_c K_{v22} \\ 0 & K_{v11} & K_{v12} \\ -K_t H_c^T & K_{v21} & K_{v22} + K_t \end{bmatrix}\begin{Bmatrix} R \\ Y_1 \\ Y_2 \end{Bmatrix} = \begin{Bmatrix} H_c M_s \\ 0 \\ M_S \end{Bmatrix}$$

4. Numerical Examples

A simply supported beam subject to two moving load. The parameters of the beam are: EI=2.5×10^{10}Nm^2, ρA=5000kg/m and L=30m.The distant between the two moving loads is 5.27m; the moving speed of the vehicle is 30m/s. And six elements are used in the calculation. The time interval is 0.01s, and t from 0 to 2. Suppose the third element is damage element. The characteristics of the vehicle model are: m_v=17.735kg, m_1=1500kg, m_2=1000kg, S=5.27m, a_1=0.519, a_2=0.481,H=1.8m, k_{s1}=2.47×10^{6}N/m, k_{s2}=4.23×10^{6}N/m, k_{t1}=3.74×10^{6}N/m, k_{t2}=4.60×10^{6}N/m, c_{s1}=3.00×10^{4}N·s/m, c_{s2}=4.00×10^4 N·s/m, c_{t1}=3.90×10^3 N·s/m, c_{t2}=4.30×10^3 N·s/m, and I_v=1.47×10^{5}kg·m^2.

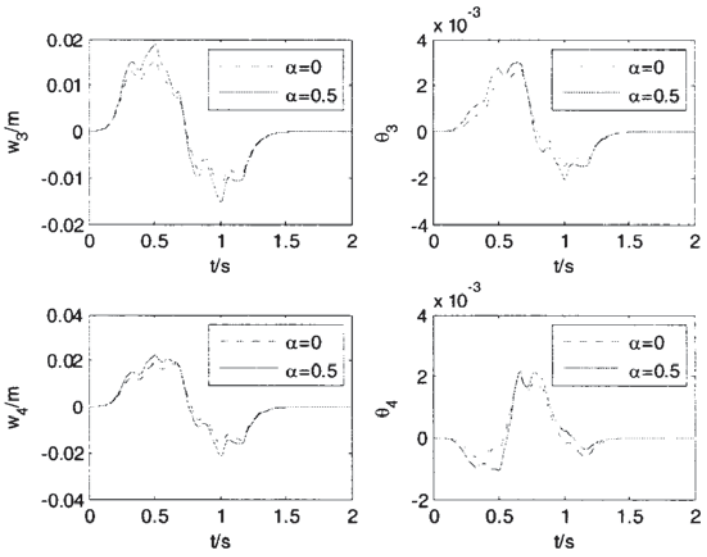

Fig.4 Dynamic response of the damage element

Figure 4 shows the dynamic response of the damage element with different damage indicators and the vehicle-bridge interaction forces are shown in Figure 5. From the results, the dynamic response and the interaction force increases with the damage.

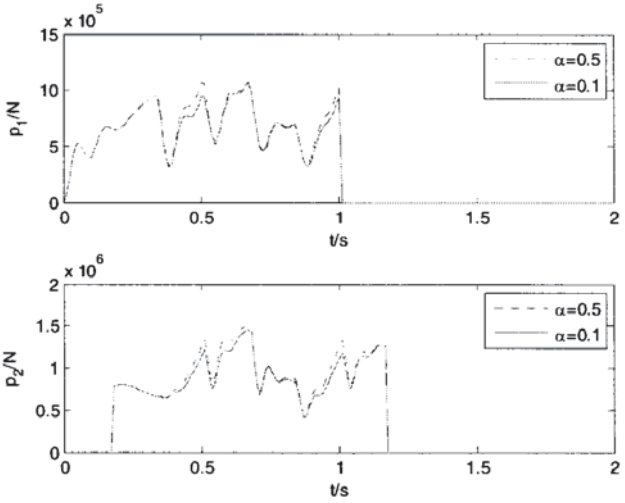

Fig.5 Vehicle-bridge interaction force

5. Conclusions

In this paper, we use a new damage beam element, modeled as a combination of a rotational spring and shear effect due to the concrete cracking and local bond deterioration of the concrete-steel interface, to analyze the non-linear dynamic behavior of damaged concrete bridge structures subject to two moving vehicular loads. With the damage index α increased, the amplitude of the vehicle-bridge interaction force and the bridge vibration response increase. Compared with the non-damage element, the amplitude of damage element changed greatly in different indicators. Further investigation is needed to fully understand the nonlinear effect of the damaged concrete beam under moving loads.

References

(1) Mazurek D.F. and Dewolf J.T. Experimental study of bridge monitoring techniques. Journal of Structural Engineering ASCE, 115(9), 1990, pp. 2532-2549.

(2) Lee H.P. and Ng T.Y. Dynamic response of a cracked beam subject to a moving load. Acta Mechanica, 106, 1994, pp.221-230.

(3) Parhi D.R. and Behera A.K. Dynamic deflection of a cracked beam with moving mass. Proceedings of the Institute of Mechanical Engineers, Part C: Journal of Mechanical Engineering Science, 211, 1997, pp.77-87.

(4) Mahmoud M.A. and Abou Zaid M.A. Dynamic response of a beam with a crack subject to a moving mass. Journal of Sound and Vibration, 256(4), 2002, pp. 591-603.

(5) Bilello C. and Bergman L.A. Vibration of damaged beams under a moving mass: theory and experimental validation. Journal of Sound and Vibration, 274(3-5), 2004, pp. 567-582.

(6) Lee J.W., Kim J.D., Yun C.B., Yi J.H. and Shim J.M. Health-monitoring method for bridges under ordinary traffic loadings. Journal of Sound and Vibration, 257(2), 2002, pp. 247-264.

(7) Majumder L. and Manohar C.S. A time-domain approach for damage detection in beam structures using vibration data with a moving oscillator as an excitation source. Journal of Sound and Vibration, 268(4), 2003, pp. 699-716.

(8) Kato,M. and Shimada,S. Vibration of PC Bridge during failure process. Journal of Structural Engineering ASCE, 112(7), 1986, pp.1692-1703.

(9) Eccles B.J., Owen J.S., Choo B.S. and Woodings Nonlinear vibrations of cracked reinforced concrete beams. Structural Dynamics---EURODYN'1999, pp.357-364.

(10) Van Den Abeele K. and De Visscher J. Damage assessment in reinforced concrete using spectral and temporal nonlinear vibration techniques. Cement and Concrete Research, 30, 2000, pp.1453-1464.

(11) Owen J.S., Eccles B.J., Choo B.S. and Woodings M.A. The application of auto-regressive time series modelling for the time-frequency analysis of civil engineering structures. Engineering Structures, 23, 2001, pp.521-536.

(12) Neild S.A., Williams M.S. and McFadden P.D. Nonlinear behaviour of reinforced concrete beams under low-amplitude cyclic and vibration loads. Engineering Structures, 24, 2002, pp.708-718.

(13) Neild S.A., Williams M.S. and McFadden P.D. Nonlinear vibration characteristics of damaged concrete beams. Journal of Structural Engineering, ASCE, 129(2), 2003; pp.260-268.

(14) Law S.S., Wu Z.M. and Chan S.L. Transverse natural vibration of a beam with an internal joint carrying in-plane flexibilities. Journal of Engineering Mechanics ASCE, 131(1), 2005, pp.80-87.

(15) Sievaselvan M.V. and Reinhorn A.N. Hysteretic models for deteriorating inelastic structures. Journal of Engineering Mechanics ASCE, 126(6), 2000, pp. 633-640.

(16) Richard R.M. and Abbott B.J. Versatile elastic-plastic stress-strain formula. Journal of Engineering Mechanics ASCE, 101(4), 1975, 511-515.

(17) Law S.S. and Zhu X.Q. Nonlinear characteristics of damage concrete structures under moving vehicular loads. Journal of Structural Engineering ASCE, 131(8), 2005, pp. 1277-1285.

(18) Henchi K., Fafard M., Talbot M. and Dhatt G. An efficient algorithm for dynamic analysis of bridges under moving vehicles using a coupled modal and physical components approach. Journal of Sound and Vibration, 212, 1998, pp. 663-683.